unsaturated five-membered nitroxyl ring in V will be smaller than for the saturated ring. In four X-ray crystallographic studies of this nitroxyl ring, the ring was found to be planar.[17-20] Thus the comparison of results in fluid solution and in the single crystal may be more reliable for molecules containing the unsaturated nitroxyl than for molecules containing the saturated nitroxyl. If this is true, then the results obtained for V in the single crystal indicate that the species present in fluid solution is the cis isomer. One can speculate that steric effects in the crystal increase the relative stability of the trans isomer. In the single crystal the values of J for the cis isomer ranged from zero to 37 × 10^{-4} $\mathrm{cm^{-1}}$. These differences are presumably due to small differences in the overall conformation of the spin-labeled side chain. The strong solvent dependence of the value of J for V in fluid solution may indicate that different solvents stabilize slightly different conformations of the side chain.

Conclusions

Single-crystal EPR spectra of V doped into zinc tetraphenylporphyrin indicated the presence of six conformations of the molecule. The interspin distances were in the range 10.0-14.0 Å, and the electron-electron spin-spin coupling constant ranged from -81×10^{-4} to $+37 \times 10^{-4}$ $\mathrm{cm^{-1}}$. A comparison of the values of r and J with those obtained previously for similar molecules suggested that three of the conformations had a cis-imine linkage and three had a trans-imine linkage. Comparison of the values of J obtained in the single crystal with values obtained in fluid solution suggested that the isomer present in fluid solution may have a cis-imine linkage.

Acknowledgment. This work was supported in part by NIH Grant No. GM21156.

Registry No. V, 84433-37-4.

---

(17) Boeyens, J. C. A.; Kreuger, G. J. *Acta Crystallogr., Sect. B: Struct. Crystallogr. Cryst. Chem.* **1970,** *B26,* 668-672.
(18) Turley, W.; Boer, F. P. *Acta Crystallogr., Sect. B: Struct. Crystallogr. Cryst. Chem.* **1972,** *B28,* 1641-1644.
(19) Alcock, N. W.; Golding, B. T.; Ioannou, P. V.; Sawyer, J. F. *Tetrahedron* **1977,** *33,* 2969-2980.
(20) Bordeaux, D.; d'Assenza, G. *Cryst. Struct. Commun.* **1978,** *7,* 409-412.

Contribution from the Department of Chemistry,
Montana State University, Bozeman, Montana 59717

Proton Transfer and Nucleophilic Displacement Reactions of Copper(II) *N,N'*-Diglycylethylenediaminate

P. K. MITCHELL and GORDON K. PAGENKOPF*

Received June 23, 1983

The reaction of $\mathrm{CuH_{-2}DGEN}$ with TRIEN and EDTA proceeds through nucleophilic and proton-transfer-limited pathways. The rate constant with trien (650 $\mathrm{M^{-1}\,s^{-1}}$) is more than 4 orders of magnitude less than that observed for the analogous triglycine complex, but the reaction with $\mathrm{H_3O^+}$ ($k = 1.6 \times 10^7$ $\mathrm{M^{-1}\,s^{-1}}$) is similar to that observed for other copper polypeptide complexes.

Introduction

Copper(II) reacts with *N,N'*-diglycylethylenediamine in basic solution to form a neutral complex in which the two amide protons are ionized.[1] The mode of coordination of the ligand to copper is through the two terminal amine groups and the two deprotonated amide nitrogens. The deprotonated complex is designated as $\mathrm{CuH_{-2}DGEN}$ (structure I). Deprotonation is virtually complete above pH 9.

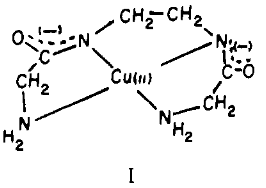

I

The displacement of short-chain polypeptide complexes from nickel(II) and copper(II) by multidentate ligands such as triethylenetetramine (TRIEN) and ethylenediaminetetraacetate (EDTA) proceeds through a number of parallel paths. These can be dissociative,[2,3] proton-transfer limited,[2-5] proton-transfer assisted,[5-9] and nucleophilic.[8,10,11]

The kinetics and mechanism for the reactions of $\mathrm{CuH_{-2}DGEN}$ with TRIEN and EDTA have been investigated in this study. The reactions exhibit several parallel paths, which include dissociative, general-acid catalytic, and nucleophilic routes.

Experimental Section

Diglycylethylenediamine was synthesized by the method of Gill and Cottrell.[12] The melting point of the dihydrochloride salt was 246 °C. A stock copper solution, 0.0975 M, was prepared from twice recrystallized $\mathrm{Cu(ClO_4)_2}$ and standardized by EDTA titration. Ionic strength was maintained at 0.10 M with $\mathrm{NaClO_4}$. Sodium borate and Tris were used to maintain constant pH. pH values were converted to hydrogen ion concentration with the extended Debye-Hückel relationship.

Solutions of $\mathrm{CuH_{-2}DGEN}$ were prepared by dissolving an analytically weighed portion of DGEN in double-distilled water followed

---

(1) Bai, K. S.; Martell, A. E. *J. Am. Chem. Soc.* **1969,** *91,* 4412.
(2) Pagenkopf, G. K.; Margerum, D. W. *J. Am. Chem. Soc.* **1968,** *90,* 6963.
(3) Billo, E. J.; Margerum, D. W. *J. Am. Chem. Soc.* **1970,** *92,* 6811.
(4) Paniago, E. B.; Margerum, D. W. *J. Am. Chem. Soc.* **1972,** *94,* 6704.
(5) Bannister, C. E.; Margerum, D. W.; Raycheba, J. M. T.; Wong, L. F. *Symp. Faraday Soc.* **1975,** *No. 10,* 78.
(6) Cooper, J. C.; Wong, L. F.; Venezky, D. L.; Margerum, D. W. *J. Am. Chem. Soc.* **1974,** *96,* 7560.
(7) Wong, L. F.; Cooper, J. C.; Margerum, D. W. *J. Am. Chem. Soc.* **1976,** *98,* 7268.
(8) Youngblood, M. P.; Margerum, D. W. *Inorg. Chem.* **1980,** *19,* 3072.
(9) Youngblood, M. P.; Chellappa, K. L.; Bannister, C. E.; Margerum, D. W. *Inorg. Chem.* **1981,** *20,* 1742.
(10) Pagenkopf, G. K.; Margerum, D. W. *J. Am. Chem. Soc.* **1970,** *92,* 2683.
(11) Billo, E. J.; Smith, G. F.; Margerum, D. W. *J. Am. Chem. Soc.* **1971,** *93,* 2635.
(12) Cottrell, T. L.; Gill, J. E. *J. Chem. Soc.* **1947,** 129.

0020-1669/84/1323-1330$01.50/0

Table I. Concentrations and k_{obsd} for the Reaction of TRIEN with $CuH_{-2}DGEN$[a]

pH	$10^3[TRIEN_t]$, M	k_{obsd}, s^{-1}	pH	$10^3[TRIEN_t]$, M	k_{obsd}, s^{-1}
6.64	2.31[b]	8.82	8.66	1.08	0.51
	3.85[b]	16.61		3.24	0.90
	5.40[b]	12.27		6.50	1.32
7.15	2.31[b]	3.74		8.65	1.54
	3.85[b]	4.58	9.28	1.44	0.84
	5.40	5.51		2.89	1.02
7.55	1.44	1.85		3.66	1.13
	4.32	2.46	9.94	1.44	6.92
	7.20	3.30		4.32	2.24
7.55	10.1	4.27		7.20	3.67
7.88	1.44	0.89		11.5	5.61
	4.32	1.37		14.4	6.74
	7.20	1.82		18.0	9.37
	10.1	2.62	10.45	1.44	0.99
8.40	0.77[b]	0.56		4.32	2.56
	1.54[b]	0.72		10.1	5.57
	3.08[b]	0.90		12.9	7.28
	4.62[b]	1.12		15.8	8.62

[a] $[CuH_{-2}DGEN_t] = 8.15 \times 10^{-5}$ M, except where designated otherwise. [b] $[CuH_{-2}DGEN_t] = 2.92 \times 10^{-5}$ M.

by adding an aliquot of Cu(II) stock solution. A 50% excess of DGEN was maintained. The solutions were always prepared fresh and used immediately upon preparation.

Triethylenetetramine solutions were prepared from the twice-recrystallized disulfate salt. These solutions were standardized spectrophotometrically with Cu(II) at pH 4.8 (acetate buffer). The TRIEN pK_a values used to resolve the rate constants are $pK_a(HT) = 9.74$, $pK_a(H_2T) = 9.08$, and $pK_a(H_3T) = 6.56$.[13]

The disodium salt of ethylenediaminetetraacetic acid was purified and recrystallized by the method of Blaedel and Knight.[14] A stock solution of EDTA was standardized by the $CaCO_3$ method[15] using Eriochrome Black T as the indicator. EDTA pK_a values used to resolve the rate constants are $pK_a(HY) = 10.26$ and $pK_a(H_2Y) = 6.16$.[16]

The reactions of $CuH_{-2}DGEN$ with $TRIEN_t$ and $EDTA_t$ were followed spectrophotometrically at 255 and 286 nm, respectively, with a Dionex stopped-flow spectrophotometer. Temperature was maintained at 25.0 °C. A typical reaction had $[Cu_t] = 2.9 \times 10^{-5}$ M and a displacing ligand concentration of at least 10 times this value. Under these conditions pseudo-first-order kinetics were observed. The reported rate constants were obtained from plots of $-\ln(A_\infty - A)$ vs. time and are the average of at least three kinetic runs. Extrapolation of absorbance reading to zero time agreed with the expected values, and the reaction is not influenced by the addition of excess DGEN. The resolved second-order rate constants were obtained with use of simultaneous equations and nonlinear least-squares fitting.[17]

Results

Reaction of $CuH_{-2}DGEN$ with TRIEN. The reaction of $CuH_{-2}DGEN$ with $TRIEN_t$ to form $CuTRIEN^{2+}$ when the $TRIEN_t$ concentration is more than a 10-fold excess follows the rate law shown in eq 1. The dependence of k_{obsd} on

$$-d[CuH_{-2}DGEN]/dt = k_{obsd}[CuH_{-2}DGEN] \quad (1)$$

$[TRIEN_t]$ was linear and exhibited a non-zero intercept. Plots for the pH 7.55, 7.88, 8.40, and 8.66 data are shown in Figure 1. The data for all pH values are listed in Table I. For these data

$$k_{obsd} = k_i + k_{TT}[TRIEN_t] \quad (2)$$

In general the intercept term decreases as pH increases, whereas the slopes of these plots decrease as the pH increases from 7 to 8.5 and then the slopes increase from pH 8.5 to 10.5.

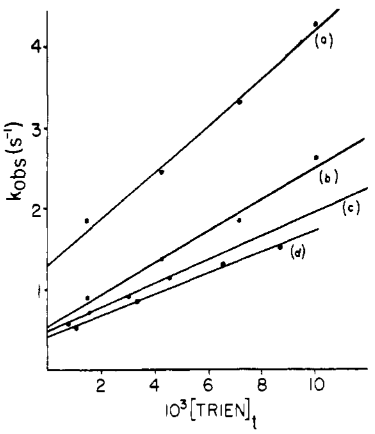

Figure 1. Dependence of k_{obsd} on $[TRIEN_t]$ at selected pH values: (a) pH 7.55; (b) pH 7.88; (c) pH 8.40; (d) pH 8.66. $[boron_t] = 5.0 \times 10^{-3}$ M.

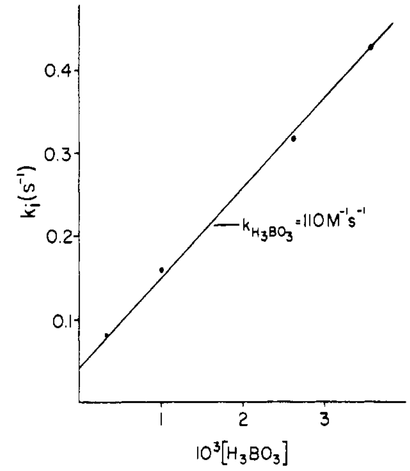

Figure 2. Resolution of the k_{H_2O} and $k_{H_3BO_3}$ contribution to k_i.

Table II. Rate Constants for the Reaction of $TRIEN_t$ with $CuH_{-2}DGEN$

constant	value
k_T	$(6.5 \pm 0.9) \times 10^2$ M^{-1} s^{-1}
k_{HT}	$(2.1 \pm 0.4) \times 10^2$ M^{-1} s^{-1}
k_{H_2T}	$(8.7 \pm 0.9) \times 10$ M^{-1} s^{-1}
k_{H_3T}	$(2.1 \pm 0.5) \times 10^3$ M^{-1} s^{-1}
k_{H_2O}	4.2×10^{-2} s^{-1}
$k_{H_3BO_3}$	$(1.1 \pm 0.1) \times 10^2$ M^{-1} s^{-1}
k_{H_3O}	$(1.5 \pm 0.3) \times 10^7$ M^{-1} s^{-1}

Over this pH range the main TRIEN species are trien, $Htrien^+$, H_2trien^{2+}, and H_3trien^{3+}. Expression of k_{TT} in terms of the rate constants for the respective TRIEN species and the fraction of the total that is present as that species results in eq 3. Solution of eq 3 for the four rate constants provides the values listed in Table II.

$$k_{TT} = k_T\alpha_T + k_{HT}\alpha_{HT} + k_{H_2T}\alpha_{H_2T} + k_{H_3T}\alpha_{H_3T} \quad (3)$$

The intercepts from plots like those shown in Figure 1 are dependent upon the H_3BO_3 and H_3O^+ concentrations (eq 4).

$$k_i = k_{H_2O} + k_{H_3BO_3}[H_3BO_3] + k_{H_3O}[H_3O^+] \quad (4)$$

Figure 2 shows the dependence on $[H_3BO_3]$. The values of k_{H_2O} and $k_{H_3BO_3}$ are also listed in Table II. The value of k_{H_3O} was obtained by plotting k_i that had been corrected for k_{H_2O} and $k_{H_3BO_3}$ as a function of hydrogen ion concentration. Data at pH 7 or less were utilized. The value of k_{H_3O} is listed in Table II.

---

(13) Smith, R. M.; Martell, A. E. "Critical Stability Constants"; Plenum Press: New York, 1975; Vol. 2.
(14) Blaedel, W. J.; Knight, H. T. *Anal. Chem.* **1954**, *26*, 741.
(15) Welcher, F. J. "The Analytical Uses of Ethylenediaminetetraacetic Acid"; Van Nostrand: Princeton, NJ, 1958.
(16) Schwarzenback, G.; Ackerman, H. *Helv. Chim. Acta* **1947**, *30*, 1798.
(17) Howald, R. A. "LIJAC Program", Montana State University, private communication, 1983.

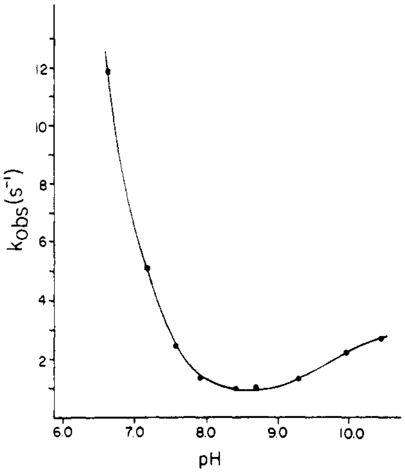

Figure 3. Agreement between predicted and observed rate constants for the reaction of $CuH_{-2}DGEN$ with $TRIEN_t$. $[TRIEN_t] = 4.32 \times 10^{-3}$ M; $[buffer_t] = 5.0 \times 10^{-3}$ M.

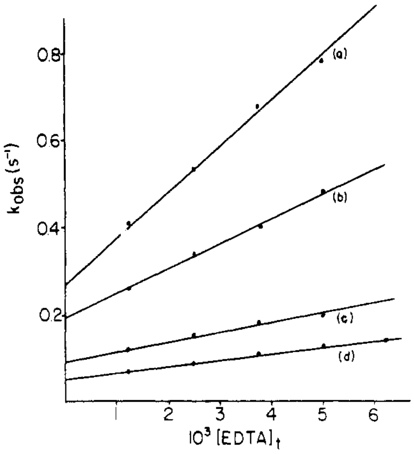

Figure 4. Dependence of k_{obsd} on $[EDTA_t]$ at selected pH values: (a) pH 9.54; (b) pH 9.98; (c) pH 10.44; (d) pH 10.96. $[boron_t] = 5.0 \times 10^{-3}$ M.

The expanded rate equation for the reaction of $TRIEN_t$ with $CuH_{-2}DGEN$ has the form

$$-d[CuH_{-2}DGEN]/dt = (k_{H_2O} + k_{H_3BO_3}[H_3BO_3] + k_{H_3O}[H_3O^+] + k_T[trien] + k_{HT}[Htrien^+] + k_{H_2T}[H_2trien^{2+}] + k_{H_3T}[H_3trien^{3+}])[CuH_{-2}DGEN] \quad (5)$$

The agreement between the observed kinetic data and the prediction values is shown in Figure 3. The solid line is predicted from the rate constants tabulated in Table II.

Reaction of $CuH_{-2}DGEN$ with EDTA. The reaction of $CuH_{-2}DGEN$ with EDTA over the pH range 7.74–10.96 under pseudo-first-order conditions is similar to that observed for the TRIEN reaction. The observed rate constants are dependent upon EDTA concentration, as shown typically in Figure 4. Slopes and intercepts from these plots decrease as the pH increases, and the kinetic data are summarized in Table III. The contribution of the various EDTA species was treated in the same manner as was done for TRIEN. For the conditions used in these experiments the contribution from k_{EDTA} was too small to measure. The values obtained for k_{HEDTA} and k_{H_2EDTA} are listed in Table IV.

The intercepts from Figure 4 are composed of k_{H_2O}, buffer constants, and hydrogen ion contribution. Values for these constants were obtained in the same manner as described for the $TRIEN_t$ reactions, and the values are summarized in Table IV. The agreement beteen observed and predicted rate constants for the EDTA displacement reaction is shown in Figure 5. The solid line is calculated. Equation 6 summarizes the expanded rate equation for the EDTA displacement reaction.

$$-d[CuH_{-2}DGEN]/dt = (k_{H_2O} + k_{H_3BO_3}[H_3BO_3] + k_{HTris}[HTris^+] + k_{H_3O}[H_3O^+] + k_{HEDTA}[HEDTA^{3-}] + k_{H_2EDTA}[H_2EDTA^{2-}])[CuH_{-2}DGEN] \quad (6)$$

Table III. Concentrations and k_{obsd} for the Reaction of EDTA with $CuH_{-2}DGEN$

pH	$10^3[EDTA_t]$, M[a]	k_{obsd}, s^{-1}	pH	$10^3[EDTA_t]$, M[a]	k_{obsd}, s^{-1}
7.74	3.75	13.2	8.96	5.00	1.82
	5.00	16.6		6.25	2.08
	6.25	21.5	9.54	1.25	0.41
8.03	1.25	2.94		2.50	0.53
	2.50	5.28		3.75	0.68
	3.75	7.62		5.00	0.78
	5.00	9.52	9.85	1.25	0.26
8.54	1.25	1.38		2.50	0.34
	2.50	2.17		3.75	0.40
	3.75	3.07		5.00	0.48
	5.00	3.56	10.44	1.25	0.121
	6.25	4.70		2.50	0.152
8.69	1.25	0.95		3.75	0.177
	2.50	1.46		5.00	0.192
	3.75	2.00	10.96	1.25	0.070
	5.00	2.46		2.50	0.084
8.96	1.25	0.74		3.75	0.110
	2.50	1.07		5.00	0.125
	3.75	1.36		6.25	0.134

[a] $[CuH_{-2}DGEN_t] = 4.38 \times 10^{-5}$ M.

Table IV. Rate Constants for the Reaction of $EDTA_t$ with $CuH_{-2}DGEN$

constant	value
k_{HEDTA}	$(5.6 \pm 1.1) \times 10$ M^{-1} s^{-1}
k_{H_2EDTA}	$(1.1 \pm 0.3) \times 10^5$ M^{-1} s^{-1}
k_{H_2O}	4.4×10^{-2} s^{-1}
$k_{H_3BO_3}$	$(1.2 \pm 0.1) \times 10^2$ M^{-1} s^{-1}
k_{HTris}	$(8.7 \pm 0.2) \times 10^2$ M^{-1} s^{-1}
k_{H_3O}	$(1.6 \pm 0.2) \times 10^7$ M^{-1} s^{-1}

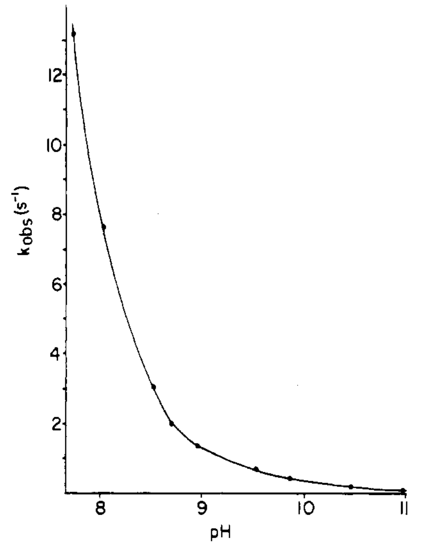

Figure 5. Agreement between predicted and observed rate constants for the reaction of $CuH_{-2}DGEN$ with $EDTA_t$. $[EDTA_t] = 3.75 \times 10^{-3}$ M; $[buffer_t] = 5.0 \times 10^{-3}$ M.

Discussion

Mechanism of Proton Transfer for $CuH_{-2}DGEN$. The rate of protonation of $CuH_{-2}DGEN$ increases as the acid strength of the proton donor increases. Figure 6 shows a plot of log k_{HA} as a function of acid strength, pK_a. The slope of the linear

Table V. Rate Constants for the Reaction of Copper(II) Complexes with TRIEN Species

complex	k_T, M^{-1} s^{-1}	k_{HT}, M^{-1} s^{-1}	k_{H_2T}, M^{-1} s^{-1}	k_{H_3T}, M^{-1} s^{-1}	ref
$Cu(H_{-2}G_3)^-$	1.7×10^7	5.1×10^6	1.2×10^5		2
$Cu(H_{-3}G_4)^{2-}$	4.9×10^2	7.1×10^1	6.2×10^1	3.7×10^2	8
$Cu(H_{-2}GGHis)^-$	0.5				6
$CuH_{-2}DGEN$	6.5×10^2	2.1×10^2	8.7×10^1	7.1×10^3	this work

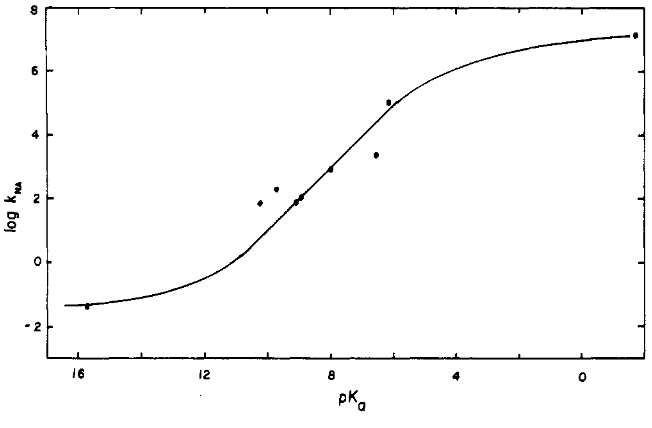

Figure 6. Brønsted plot for the reaction of $CuH_{-2}DGEN$ with acids (from left to right): H_2O, $HEDTA^{3-}$, $Htrien^+$, H_2trien^{2+}, H_3BO_3, $HTris^+$, H_2EDTA^{2-}, H_3O^+.

portion is unity and is similar in shape to that observed for other systems: $CuH_{-2}GGG^-$,[2] $CuH_{-3}GGGG^{2-}$,[8] $CuH_{-2}GGHis^-$,[6] $NiH_{-2}GGG^-$.[3] General-acid catalysis indicates that proton transfer occurs during the rate-determining step, and in this case the proton is being transferred to one of the two deprotonated imide nitrogens. The reaction sequence is shown in eq 7 and 8.

$$CuH_{-2}DGEN + HA \xrightarrow{k_{HA}} CuH_{-1}DGEN + A^- \quad (7)$$

$$CuH_{-1}DGEN + \text{nucleophile} \xrightarrow{\text{fast}} \text{products} \quad (8)$$

A characteristic of this reactivity pattern is the S-shaped Brønsted plot. The upper limit is well below diffusion-controlled rate constants, and the lower limit is controlled by the reaction with H_2O, which is a coordinating acid and thus exhibits a rate constant greater than what would be expected.

The k_{H_3O} rate constant, (1.5–1.7) × 10^7 M^{-1} s^{-1}, for $CuH_{-2}DGEN$ is similar but somewhat larger than the values observed for $CuH_{-2}GGG^-$, 1.3 × 10^7 M^{-1} s^{-1},[2] and $CuH_{-2}GGHis^-$, 1.1 × 10^7 M^{-1} s^{-1}.[6,7] For these three complexes the major difference resides within one chelate ring. This is demonstrated schematically in structures II, III, and IV for

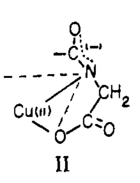

II

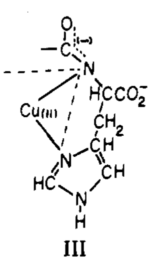

III

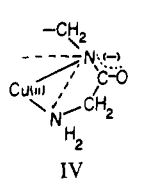

IV

GGG, GGHis, and DGEN, respectively. The most labile of the terminal groups is the carboxylate of triglycine, with the imidazole nitrogen of glycylglycylhistidine being least labile. The presence of the six-membered chelate ring in $CuH_{-2}GGHis^-$ will relieve some of the steric strain in this portion of the complex. If the nature of the protective group played a large role in determining the rate of the reaction with H_3O^+, the observed rate constants should exhibit more variation than they do. The comparable magnitude of the rate constants indicates that the work terms (W_R) are similar.[8] Apparently solvent reorganization and changes in bond length within the imide linkage upon proton transfer to the nitrogen are not largely affected by the nature of the terminal donor. This is not the case when a proton is being transferred to a terminal imide nitrogen, where in the case of $CuH_{-3}GGGG^-$ the rate constant is a factor of 10 larger. This increased rate constant can be attributed to trans labilization and chelate ring strain.[8]

The variation in the rate constants for the solvent-mediated pathway, k_{H_2O}, is much larger. For the three complexes $CuH_{-2}GGG^-$, $CuH_{-2}DGEN$, and $CuH_{-2}GGHis^-$ the values are 0.12, 0.04, and 0.000 75 s^{-1}, respectively. This decrease parallels the lability of the terminal groups and may indicate that H_2O is acting as a nucleophile; however, the comparable rate constant with $CuH_{-2}GGGG^{2-}$ is much larger,[8] 16 s^{-1}, and for this complex water is believed to be acting as a coordinating acid. In any event the solvent-mediated pathway is much more dependent upon the nature of the terminal group than the proton-transfer pathway is.

Mechanism for the Reaction of TRIEN with $CuH_{-2}DGEN$. For nucleophilic displacement of DGEN from $CuH_{-2}DGEN$ by TRIEN the order of reactivity should be trien > $Htrien^+$ > H_2trien^{2+} > H_3trien^{3+}. The order of the reactivity is, however, trien > $Htrien^+$ > H_2trien^{2+} < H_3trien^{3+} and indicates that H_3trien^{3+} and possibly H_2trien^{2+} are acting as acids. Table V summarizes the rate constants for the trien species with a sequence of analogous copper complexes. The most reactive complex is $CuH_{-2}GGG^-$ and the least reactive is $CuH_{-2}GGHis^-$. For these reactions the critical step involves coordination of trien to a vacated planar position. In the case of triglycine the carboxylate donor is sufficiently labile to provide a vacant site. For $GGHis^-$ an imidazole nitrogen occupies the fourth planar site. This coordination is much less labile, and as a consequence the rate of reaction with trien is reduced by nearly 8 orders of magnitude. The other two ligands, tetraglycine and DGEN, have imide and amine nitrogen coordination, respectively, at the fourth planar site. These two groups are not as labile as the carboxylate donor, and thus there is sizable reduction in the rate constants. They are more labile than the imidazole grouping, however. Studies with $NiH_{-2}DGEN$[18] indicate that positioning of the planar NCO linkage on both sides of the square-planar complex impart sufficient kinetic stability to cause a shift in the position of the rate-determining step.

The decrease in reactivity of $Htrien^+$ as compared to trien is a factor of 3 for both the $CuH_{-2}DGEN$ and $CuH_{-2}GGG^-$ complexes. The decrease is somewhat larger than the 36% expected from the distribution of protons in $Htrien^+$.[19] As the protonation level of trien increases, the rate constants decrease but the decrease for $CuH_{-2}DGEN$ is not as great as would be expected if H_2trien^{2+} were acting as a nucleophile. As a consequence H_2trien^{2+} is believed to be acting as a general acid in the ligand-exchange reaction. The fact that k_{H_3T} is larger than k_{H_2T} for the reaction with $CuH_{-2}DGEN$ is consistent with this reactivity pattern. The rate constant for H_2trien^{2+} fits the Brønsted plot very well (Figure 6), but the value for H_3trien^{3+} seems to be too low by a factor of about

---

(18) Storvick, J. P. Masters Thesis, Montana State University, Bozeman, MT, 1981.

(19) Sudmeier, J. L.; Reilley, C. N. *Anal. Chem.* **1964**, *36*, 1698.

3. No loss of TRIEN dependence was observed at high concentration in these studies, and thus it is concluded that the proton-assisted nucleophilic displacement is not a major contributor. For this pathway to be operative, the lability of the termain group would have to be reduced sufficiently to stabilize outside protonation of the imide linkage. Coordination of the imidazole nitrogen in $CuH_{-2}GGHis^-$ achieves this whereas the carboxylate donor in $CuH_{-2}GGG^-$ is too labile. These studies indicate that the terminal amine coordination in $CuH_{-2}DGEN$ is also too labile and general-acid catalysis is the observed reaction for H_3trien^{3+} and H_2trien^{2+}.

Mechanism for the Reaction of EDTA with $CuH_{-2}DGEN$. $EDTA^{4-}$ in general is not a good nucleophilic ligand for the replacement of polypeptide ligands from the copper(II) and nickel(II) complexes. This is observed in these studies, where k_{EDTA} is too small to be determined. Values were obtained for the two protonated species $HEDTA^{3-}$ and H_2EDTA^{2-} and are consistent with these two ligands acting as acids. These ligands may act as coordinating acids and as a consequence exhibit larger rate constants than expected. This does not appear to be the case for H_2EDTA^{2-} but may be for $HEDTA^{3-}$.

Conclusions

The reaction of $CuH_{-2}DGEN$ with TRIEN and EDTA proceeds through nucleophilic and proton-transfer-limited pathways. The presence of terminal amine groups reduces the reactivity through the nucleophilic and solvent-assisted pathways as compared to that for the similar copper–triclycine complex. This is not the case for the proton-transfer reaction, where the rate constants are comparable to those observed for the other analogous polypeptide complexes.

Registry No. $CuH_{-2}DGEN$, 15156-44-2; trien, 112-24-3; EDTA, 60-00-4.

Contribution from the Department of Chemistry,
Texas A&M University, College Station, Texas 77843

Thermodynamic Study and Stabilities of Complex Dicerium Carbide Molecules

J. E. KINGCADE, JR., D. L. COCKE, and K. A. GINGERICH*

Received February 10, 1983

The composition of the vapor phase above the cerium–graphite system was investigated in the temperature range 2100–2800 K by means of Knudsen-effusion mass spectrometry. The molecules Ce, Ce_2C, Ce_2C_2, Ce_2C_3, Ce_2C_4, Ce_2C_5, and Ce_2C_6 were shown to exist in the vapor phase above the liquid solution. Third-law enthalpy changes were evaluated for the following equilibrium reactions: $Ce_2C_n(g) = 2Ce(g) + nC(graph)$. These values were then combined with ancillary literature data to give the atomization energies, $\Delta H_a{}^\circ{}_0$ (kJ mol^{-1}), and the standard enthalpies of formation, $\Delta H_f{}^\circ{}_{298.15}$ (kJ mol^{-1}), of the various polyatomic carbide molecules: Ce_2C, 1047 ± 26, 506 ± 26; Ce_2C_2, 1690 ± 25, 576 ± 25; Ce_2C_3, 2332 ± 28, 647 ± 28; Ce_2C_4, 3076 ± 25, 615 ± 25; Ce_2C_5, 3654 ± 32, 750 ± 32; Ce_2C_6, 4347 ± 36, 770 ± 36.

Introduction

Experimental investigations of the equilibrium vapor above metal–graphite systems by Knudsen cell mass spectrometry over the last two decades have resulted in the thermodynamic characterization of a number of stable gaseous carbides. These have been reviewed in several summaries.[1–4] More recent investigations have shown that the metal carbide vapors are surprisingly quite complex in composition and may contain polyatomic metal carbide species with up to nine atoms.[5–9]

Except for a few preliminary reports,[5,7c,10] very little is known about dimetal carbides of electropositive transition metals. Only the molecules Ce_2C_n (n = 1–6), La_2C_n (n = 1–6), and Ti_2C_4 have been observed and their approximate atomization energies presented. The molecules M_2C_4 are found to have a vapor concentration approximately equal to that of the penta- and hexacarbides. The concentrations of the remaining dimetal carbides are approximately an order of magnitude less than the concentrations of the dimetal tetracarbides.

The above examples amply demonstrate the very complex nature of the vapors above electropositive transition-metal–graphite systems at high temperatures. It is seen in numerous instances that if a stable dicarbide exists, a whole series of metal–carbon species may be observed of the type MC_n and M_2C_n at high temperatures. The knowledge of the vapor composition is functional to the description of the vaporization thermodynamics of any system and is of considerable technological and scientific interest.

As part of our continued research concerned with the identification and the thermodynamic properties of gaseous carbide systems, we have investigated the system cerium–carbon by Knudsen-effusion mass spectrometry. We have previously reported and evaluated thermodynamic values for the gaseous monocerium carbides, within the temperature range 2100–2800 K.[5] The following report is a discussion of the observed gaseous dicerium carbides, which we observed at the higher temperatures in conjunction with previously reported molecules.

Experimental Section

The mass spectrometer employed for this investigation is a single-focusing, 12-in. radius, magnetic deflection, 90° sector, Knudsen cell, high-temperature instrument (Nuclide Model 12-90-HT). The general methods of high-temperature Knudsen-effusion mass spectrometry have been presented in several reviews.[3,11,12] The specific mass spectrometer and experimental arrangements are described more

---

(1) DeMaria, G. In "Chemical and Mechanical Behavior of Inorganic Materials"; Searcy, A. W., Ragone, D. V., Colombo U., Eds.; Wiley-Interscience: New York, 1970; pp 81–105.

(2) DeMaria, G.; Balducci, G. *Int. Rev. Sci.: Phys. Chem., Ser. One* **1972**, *10*, 209.

(3) Gingerich, K. A. *Curr. Top. Mater. Sci.* **1980**, *6*, 345.

(4) Storms, E. K. "The Refractory Carbides"; Academic Press: New York, 1967.

(5) (a) Kingcade, J. E.; Cocke, D. L.; Gingerich, K. A. *Inorg. Chim. Acta* **1976**, *17*, L1; (b) *High Temp. Sci.* **1983**, *16*, 89.

(6) Gingerich, K. A.; Haque, R.; *J. Chem. Soc., Faraday Trans. 2* **1980**, 101.

(7) (a) Gupta, S. K.; Gingerich, K. A. *J. Chem. Phys.* **1979**, *71*, 3072; (b) **1980**, *72*, 2795; (c) *High Temp. High Pressures* **1980**, *12*, 273.

(8) Hague, R.; Gingerich, K. A. *J. Chem. Phys.* **1981**, *74*, 6407.

(9) Gingerich, K. A.; Pelino, M.; Hague, R. *High Temp. Sci.* **1981**, *14*, 137; *J. Chem. Soc., Faraday Trans. 1*, **1982**, 341.

(10) Gingerich, K. A.; Nappi, B. N.; Hague, R.; Pelino, M. *Inorg. Chim. Acta* **1981**, *54*, L141.

(11) Grimley, R. T. In "Characterization of High Temperature Vapors"; Margrave, J. L., Ed.; Wiley-Interscience: New York, 1967; pp 195–243.

(12) Drowart, J.; Goldfinger, P. *Angew. Chem.* **1967**, *79*, 589; *Angew Chem., Int. Ed. Engl.* **1967**, *6*, 581.

0020-1669/84/1323-1334$01.50/0